Origin of tourmaline-rich rocks in a Paleoproterozoic terrene(N.E.China): Evidence for evaporite-derived boron

XU Hong[1], PENG Qi-ming[2], Martin R. Palmer[3]

(1.*China University of Geosciences, Beijing* 100083, *China;* 2. *China Geological Survey, Beijing* 100011, *China;* 3. *School of Ocean & Earth Science, University of Southampton, UK*)

Abstract: We have analysed the major element, trace element and boron isotope composition of borates, tourmaline-rich rocks and their non-tourmalinised equivalents from the lower portion of the Paleoproterozoic South Liaohe Group (N.E. China). These rocks host economically important borate deposits that formed in an evaporitic environment. The sequence contains abundant tourmaline in leptynites, stratiform tourmalinites, quartz-tourmaline veins and pegmatites that have spatial and temporal relationships to the borates.Tourmalines distal to the borates have lower $\delta^{11}B$ values (−5.2 ‰ to +3.6 ‰) than those proximal to the borates (+1.8 ‰ to +9.4 ‰)that are slightly lower than those of the borates (av. +10.5 ‰). Mg/Fe ratios of the distal tourmalines are low (<1.0) relative to proximal tourmaline-rich rocks (>1 to 2.6). These differences reflect the fact that the evaporites are a major source of B and Mg. The geochemistry of immobile elements in the stratiform tourmalinites is similar to that of their unmineralised equivalents (interpreted as meta-tuffites), suggesting that the tourmalinites formed via alteration of Al-rich tuff layers by boron-rich fluids derived from leaching of the underlying borates. Field evidence and geochemical data support a three-stage model of tourmaline formation. The first stage was coeval with deposition of the borates, during which boron from hot springs was adsorbed by clay minerals in the tuffs that were later metamorphosed to tourmaline-bearing leptynites. In the second stage, hot fluids leached boron from the evaporites and passed through overlying tuffs to form the stratiform tourmalinites. During later emplacement of granites at the base of the sequence, felsic veins and pegmatites intruded the borates and tourmalinites. Boron from the borates diffused into the felsic veins, forming coarse-grained tourmaline at their margins. This association of tourmaline with the borate deposits emphasizes the significance of tourmaline-rich rocks as a prospecting guide for borates in this area and has implications for the origin of tourmalinites in other metamorphic terrenes.

Key words: tourmaline; borates; Paleoproterozoic; evaporite; Liaoning

0 Introduction

The origin and significance of tourmaline-rich rocks in metamorphic terrenes, especially those associated with SEDEX-type massive sulphide deposits, are of interest to both petrologists and economic geologists. The geology, geochemistry and boron isotope composition of these rocks provide information concerning the nature of the hydrothermal fluids responsible for their formation and the depositional environment and has significance for the origin of associated ore deposits[1-5].

The Paleoproterozoic borate deposits of Liaoning and Jilin Provinces are the major boron source in China. They are unusual in that all the world's other major borate deposits are located in Neogene (or younger) sediments[6]. Early studies suggested the Liaoning borates were skarns[7], or metamorphosed volcano-sedimentary deposit[8-9], but recent work suggests they are metamorphosed evaporites in which the borates were originally present as evaporite minerals[10-12].

There is a close spatial association between the borates and tourmaline-rich rocks in the area, providing an opportunity to test the genetic link between these rocks, which has been inferred in other geological settings[2,5,13]. In Liaoning, tourmaline is present in stratiform tourmalinites, tourmaline-bearing leptynites,

收稿日期:2004-05-16;**改回日期**:2004-06-12

基金项目:国家自然科学基金(49573175,40373023)和英国皇家学会中英合作项目联合资助。

作者简介:许虹,女,1958 年生,副教授,从事结晶学、矿物学及找矿矿物学、成因矿物学和环境矿物学方面的研究;E-mail:hongx88@sohu.com。

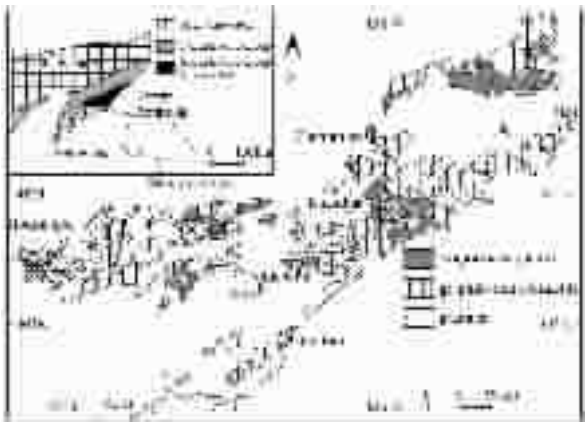

Fig. 1 Regional geology of the borate deposits in Liaoning and Jilin Provinces, China. The upper left insertion shows the tectonic location of the South Liaohe Group that hosts the borate deposits (modified after Zhang[15], 1984)

tourmaline-quartz veins and pegmatites. An association of tourmaline with local granites has been used to suggest that the borate deposits are related to emplacement of these granites[7,14]. To test this hypothesis we have carried out a chemical and isotopic study of the tourmaline-rich rocks. This work has relevance to studies of metamorphosed evaporites and tourmalinites elsewhere in the world.

1 Geological setting

The Paleoproterozoic South Liaohe and Jian Groups in Liaoning and Jilin Provinces form an east-west striking volcano-sedimentary sequence that extends for 300 km (Fig. 1). To the north it is bounded by a fault contact with the North Liaohe Group. The sequence is interpreted as a paleo-rift system in an Archean greenstone belt [15-16] filled with sediments 2 300 Ma old [17-18]. Recently, Peng and Palmer (1998)proposed a post-collision model for the Paleoproterozoic tectonics.

The stratigraphy of the Liaoning borate deposits has been described by Peng and Palmer[12,19]. Briefly, the sequence comprises (in ascending order) four major lithologic units (Fig.2): (unit 1) magnetite-microcline rocks, (unit 2) biotite leptynites, (unit 3) tourmaline-bearing or tourmaline-rich leptynites with intercalations of borate-hosting magnesian marbles, and (unit 4) magnetite- or rutile-bearing leptites. Amphibolite lenses are intercalated within all the units. The magnesite and/or dolomitic carbonates are the exclusive host of the borates and are often altered to diopside- and forsterite-bearing rocks. The main borate minerals are suanite, szaibelyite and ludwigite.

The magnetite-microcline rocks are interpreted as metamorphosed red beds formed in an arid environment[10-12,19]. The leptynites and leptites have high levels of Na, K and B. Their chemistry and zoning are similar to volcanic tuffs altered in a saline lake setting [20], compatible with the hypothesis of an arid depositional setting for the base of the Liaohe Group [12,19]. The evaporitic sequence is overlain by graphite-rich metasediments of the Gaojiayu Formation. The South Liaohe Group experienced amphibolite-facies metamorphism and strong, multiple deformation at 2 100~2 000 Ma, and was intruded by A-type granites ~1 900 Ma [9,15,17].

Table 1 Geological characteristics of tourmaline-rich and tourmaline-bearing rocks in Liaoning and Jilin Provinces

	Occurrences	Structures and textures	Mineralogy
Stratiform Tourmalinites	In unit 3,restricted within the range of borates; occur as hanging walls of the borates, hosted mostly in biotite leptynites; lenticular, up to 200 m along strike	Banded structures with relict beddings similar to those of the host rocks; tourmaline shows metamorphic textures and the c-axis of tourmaline parallel to S_1	Tourmaline accounts for 20%—90%;the associated minerals are Quartz, biotite and feldspars, which are dependent upon the host lithology; other accessory minerals are similar to their host rocks but lack magnetite and ilmenite
Tourmaline-leptynites	Hosting borates; up to tens of metres thick and can be traced for kilometers along strike; they are stratigraphically equivalent to the stratiform tourmalinites and a mark layer of unit 3	Striking beddings expressed by biotite, amphiboles and tourmaline bands, parallel to S_1 in most places except in fold hinges; the minerals exhibit granoblastic texture; tourmaline can either be inclusions in quartz and feldspars or encloses the latter to form poikiblastic texture	Quartz,K-feldspar or albite,with or without plagiocalse, dark colored minerals include biotite,tremolite/diopside or hornblend/hend-bergite;tourmaline may account for <5% to up to 20%;accessory minerals include magnetite, ilmnite,zircon, sphene, and apatite, etc..
Tourmaline veins	Crosscutting characteristically the borates-carbonates; also found in amphibolites; small size; usually occur near pegmatites	Crosscutting S_1, as veinlets, irregular veins or disseminations in the host rocks; tourmaline grains and associated quartz+feldspars are not deformed	Tourmaline is associated with tremolite, phlogopite (in carbonates) or actinolite (in amphibolites);with or without quartz
Tourmaline pegmalites	Can crosscut a variety of lithologies,but more commomly occur within or adjacent to the borate-carbonates; tourmaline often occurs at the margins of pegmatites	Crosscutting S_1, as veins or stockworks; tourmaline coarser than other categories; no preferred orientation	Relatively simple mineralogy, dominated by tourmaline, quartz and feldspars

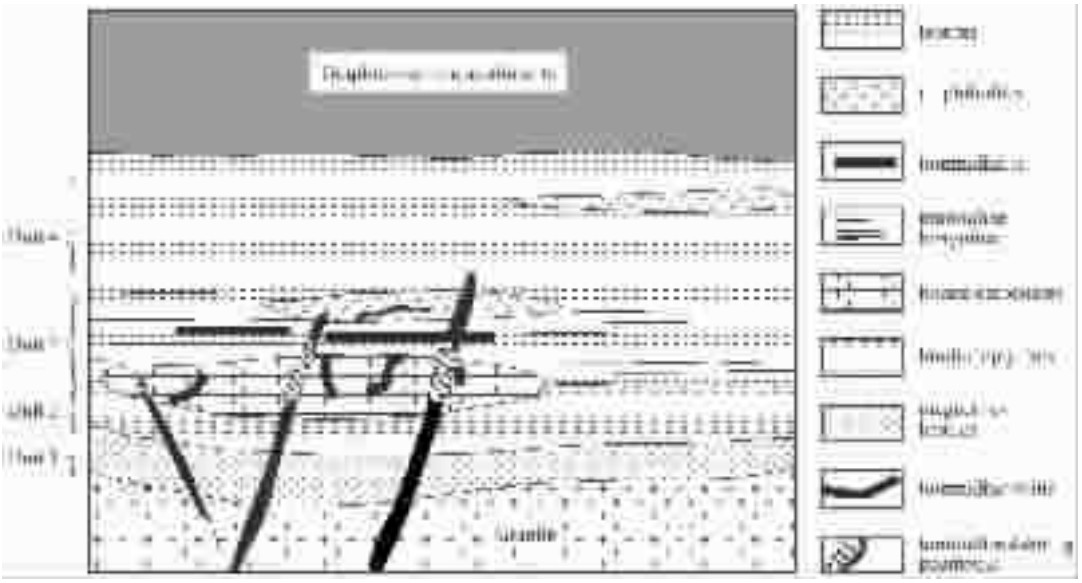

Fig.2 Stratigraphic sequence of the borate-hosting sequence and occurrences of tourmaline-rich rocks (not to scale)

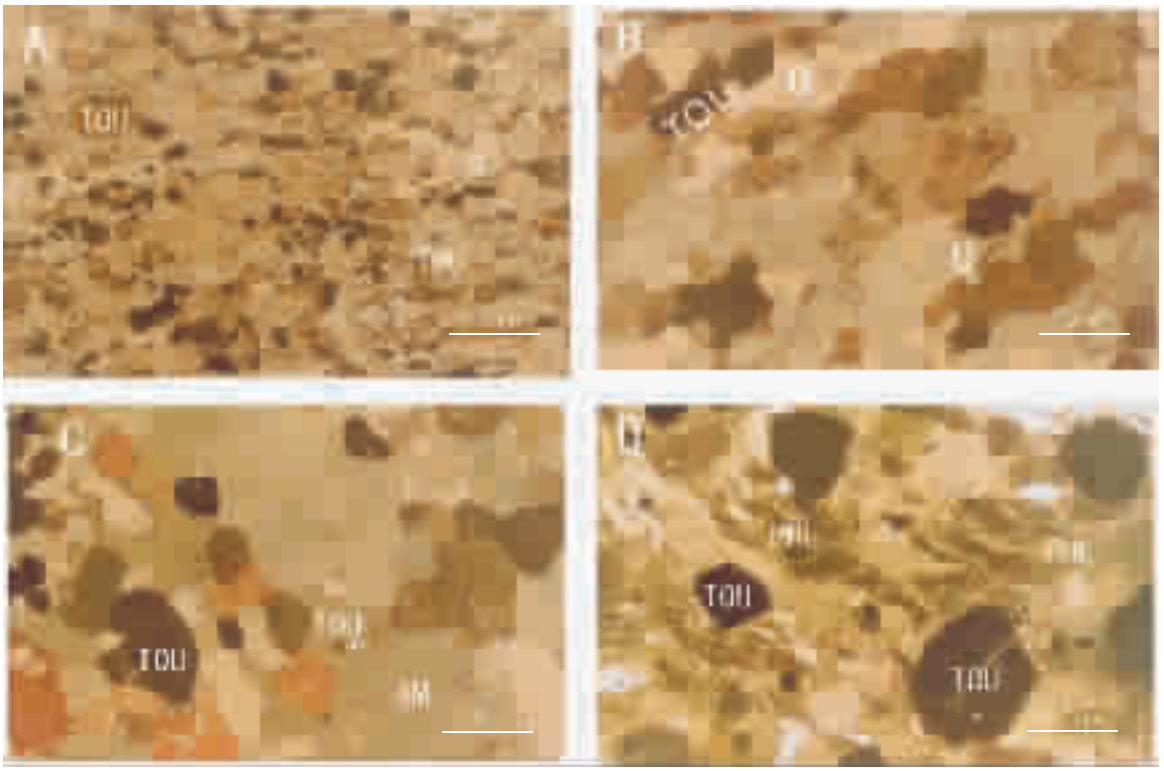

Fig. 3 Microphotographs of tourmaline-rich rocks

A- Tourmaline-leptynite away from borates (LN-14), the fine-grained tourmaline is enclosed by quartz, feldspar and coarser tourmaline overgrowth; B-Tourmalinite from immediate hanging wall of borate (HX-25); C-Tourmalinisation in amphibolite (from Wengquangou); D-Tourmaline-phlogopite rock adjacent to pegmatite that crosscuts borate-carbonate (H5-92). Width of view field 4 mm, plane-polarized light. Mineral symbols: Q=quartz, TOU=tourmaline, AM=amphibol, PHL=phlogopite, MIC=microcline

2 Occurrences and petrography of tourmaline-rich rocks

Within the study area, tourmaline-rich rocks can be broadly classified as stratiform tourmalinites and tourmaline-rich leptynites, discordant veins and pegmatites (Table 1).These rock types are hosted by various lithologies, but are most common in unit 3 where they have a close spatial association with the borates.

2.1 Stratiform tourmalinites and tourmaline -bearing leptynites

These rocks can be discontinuously traced for >100 km, but they are most abundant in the immediate area of the borates. The host rocks of the tourmalinites are dominated by biotite-leptynites and, less commonly, amphibole (tremolite)-leptynites. Thick tourmalinite layers (up to 90% tourmaline) are only found in the direct hanging walls of the borates and tourmaline concentrations in the rocks decrease away from the borates. This close association has led to the use of tourmaline as a prospecting guide for blind borate bodies (J.D. Liu, 1992, pers. comm.).

The leptynites have a banded structure[12]that is most compatible with a sedimentary origin. The leptynites mineralogy consists mainly of feldspar, quartz, biotite or amphibolite and variable amounts of magnetite. The tourmaline-rich bands are hosted conformably in the leptynites and have sharp upper and lower contacts with their host rocks [10]. The tourmaline bands show the same folding as the biotite and amphibole bands in their host rocks, and there are no penetrative tourmaline veinlets that may suggest channel-ways for boron-rich fluids in the fold hinges. This suggests a pre- or syn-metamorphic precipitation of tourmaline.

In tourmaline-leptynites (<10% tourmaline), tourmaline occurs either as small inclusions (50 μm) within, or as poikiloblastic grains intergrown with quartz and feldspars (Fig.3-A). The tourmaline grain size increases with increasing tourmaline enrichment, and it more commonly exhibits poikiloblastic textures enclosing feldspars and quartz (Fig.3-B). Metamorphic recrystallisation of the tourmaline is suggested by the poikiloblastic texture and grain boundaries (Fig.3 -B). Tourmaline is generally associated with quartz, and the contents of feldspars and dark minerals (biotite and/or amphiboles) generally decrease with increasing tourmaline enrichment. In highly enriched tourmalinites (dominated by tourmaline and quartz), feldspars (mostly microcline) are enclosed in tourmaline and quartz as relics.

There are striking similarities in mineralogy between the tourmaline-rich rocks and the host leptynites. The species of dark minerals (biotite, tremolite etc.), feldspars (albite or microcline) and accessory minerals (zircon and apatite) in the tourmaline -rich bands are identical to those in the untourmalinised equivalents, even when tourmaline enrichment is >50%.

2.2 Tourmaline-rich veins and pegmatites

Tourmaline-bearing quartz veins and pegmatites crosscut a variety of lithologic units, but they are generally restricted to the borate bodies or their stratigraphic hangingwall. Within these occurrences tourmaline is usually present as rims to the veins and is only abundant in veins and pegmatites that crosscut the borates or borate-bearing carbonates and calc-silicates [12]. Tourmaline alteration is present adjacent to these veins in amphibolites and calc-silicates, mostly as irregular veinlets. Within the amphibolites, the alteration is characterised by replacement of hornblende and plagioclase by actinolite and tourmaline (Fig.3-C). In the calc-silicates and marbles, tourmaline is associated with phlogopite or actinolite/tremolite (Fig.3-D).

3 Tourmaline chemistry

Tourmaline was analysed by wavelength-dispersive electron microprobe methods for 11 major and minor elements. The analyses were carried out at Bristol, using a JEOL-8 600 Superprobe coupled with a Link computer. Operating conditions were: accelerating voltage 15 kV, beam current 15 nA, and counting times 15 sec on peak, 8 sec on background. Corrections were made with the ZAF method. Standards used were natural minerals and synthetic compounds, including SiO_2 (Si), $MgAl_2O_4$ (Al), $SrTiO_3$ (Ti), Fe_2O_3 (Fe), olivine (Mg), MnO (Mn), $CaSiO_3$ (Ca), albite (Na), adularia (K), MgF_2 (F), and a pantellerite glass (Cl). The beam was tightly focused to a 1-2 μm spot. The 95 analyses that were performed on 15 samples cover most of the different occurrences of the tourmalinites and tourmaline-bearing rocks.

The tourmalines lie along the schorl-dravite solid solution series (Table 2). On $Al-Al_{50}Fe_{50}-Al_{50}Mg_{50}$ and Ca-Fe-Mg ternary plots the data fall closer to the dravite end member (Fig.4). The largest chemical variations occur in the Mg/Fe ratios, and less significantly, K/Na ratios (Table 2). In general, the distal tourmaline-leptynites have lower Mg/Fe ratios than the proximal tourmalinites (up to 2.6). High Mg/Fe ratios are also characteristic of the tourmaline veins in and/or overlying the borates and magnesian carbonates (1.2~ 2.6). The K/Na ratios are a function of their host lithologies. The tourmalines hosted in microcline-

Table 2 Microprobe analysis of tourmaline (%)

	FJ-8		FJ-5		LA-12	H1-43	HX-25		H5-92		FJ-2	H4-39		H5-112
	core (4)*	rim (4)	core (2)	rim (3)	average (3)	average(4)	core (4)	rim (4)	core (3)	rim (3)	average (3)	core (3)	rim (2)	average(6)
Na_2O	2.385**	2.031	1.603	1.617	1.339	2.579	1.825	1.805	1.73	1.459	2.323	1.763	1.589	1.573
	(2.314-2.450)	(1.985-2.065)	(1.584-1.623)	(1.550-1.678)	(1.311-1.367)	(2.573-2.606)	(1.804-1.846)	(1.601-1.809)	(1.594-1.774)	(1.300-1.489)	(2.288-2.359)	(1.684-1.842)	(1.51-1.669)	(1.552-1.866)
MgO	4.447	6.27	9.241	8.941	9.110	8.396	8.061	8.686	7.989	8.206	6.955	8.566	9.23	7.53
	(3.898-4.925)	(6.230-6.316)	(9.1823-9.300)	(8.884-8.993)	(9.038-9.167)	(8.255-8.537)	(8.056-9.915)	(8.100-9.598)	(7.897-8.081)	(8.165-8.530)	(6.915-6.996)	(7.799-9.333)	(9.197-9.264)	(7.259-7.886)
SiO_2	35.479	35.587	34.694	34.725	35.39	36.381	35.847	36.168	36.083	35.524	37.286	36.086	36.219	35.523
	(35.074-35.986)	(35.479-35.681)	(34.541-34.847)	(34.590-34.992)	(35.291-35.912)	(36.270-36.460)	(35.790-36.072)	(35.836-36.500)	(35.686-36.269)	(35.523-35.951)	(37.205-37.367)	(36.001-36.451)	(36.045-36.394)	(35.277-35.917)
Al_2O_3	29.843	30.082	18.175	16.351	22.674	26.536	26.155	26.215	28.646	28.286	24.520	27.282	26.378	28.068
	(29.602-30.231)	(29.834-30.281)	(7.707-18.608)	(15.545-17.754)	(22.395-22.945)	(26.498-26.753)	(25.824-26.989)	(25.722-26.295)	(28.576-28.713)	(27.695-28.362)	(24.269-24.772)	(26.237-28.328)	(26.369-26.386)	(27.105-28.586)
K_2O	0.086	0.102	0.269	0.272	0.107	0.042	0.067	0.053	0.097	0.123	0.088	0.107	0.068	0.102
	(0.069-0.108)	(0.082-0.120)	(0.2575-0.280)	(0.263-0.285)	(0.0938-0.125)	(0.028-0.050)	(0.031-0.071)	(0.045-0.060)	(0.087-0.108)	(0.113-0.492)	(0.069-0.107)	(0.079-0.133)	(0.064-0.072)	(0.08-0.144)
CaO	0.419	1.199	2.108	2.030	2.872	0.705	2.094	2.079	1.93	2.524	0.928	2.11	2.445	2.159
	(0.289-0.520)	(1.167-1.223)	(2.102-2.114)	(1.884-2.126)	(2.786-2.928)	(0.518-0.754)	(1.992-2.138)	(2.032-2.443)	(1.834-2.231)	(2.410-2.638)	(0.849-1.008)	(1.921-2.300)	(2.365-2.525)	(1.723-2.200)
TiO_2	0.594	0.802	1.611	10595	1.673	1.264	0.927	0.93	0.297	0.266	1.210	0.45	0.669	0.477
	(0.377-0.855)	(0.761-0.866)	(1.588-1.633)	(1.585-1.602)	(1.688-1.694)	(1.213-1.377)	(0.884-1.248)	(0.815-1.059)	(0.269-0.324)	(0.265-0.281)	(1.195-1.226)	(0.201-0.699)	(0.654-0.684)	(0.277-0.902)
FeO	12.894	10.100	18.136	20.009	12.607	10.247	11.334	10.615	9.683	9.693	13.310	10.073	9.58	11.212
	(9.756-10.356)	(9.756-10.356)	(17.136-18.683)	(18.355-20.924)	(12.197-12.909)	(9.875-10.250)	(7.333-11.632)	(9.670-11.556)	(9.610-9.812)	(9.668-9.959)	(13.277-13.343)	(9.626-10.344)	(9.563-9.589)	(10.1307-11.475)
MnO	0.03	0.068	0.099	0.059	0.003	0.012	0.05	0.031	0.03	0.044	0.051	0.048	0.024	0.019
	(0.012-0.060)	(0.03-0.107)	(0.074-0.124)	(0.007-0.119)	(0.00-0.005)	(0.00-0.055)	(0.011-0.095)	(0.013-0.062)	(0.00-0.059)	(0.00-0.089)	(0.025-0.077)	(0.00-0.0690)	(0.018-0.031)	(0.007-0.062)
Total	86.138	86.203	85.88	85.58	85.535	86.15	86.31	86.503	86.455	86.31	86.66	86.44	86.18	86.645
	(85.86-86.40)	(85.83-86.44)	(85.83-85.93)	(85.52-85.69)	(85.53-85.85)	(85.88-86.24)	(85.4-96.6)	(86.33-86.77)	(86.27-86.52)	(86.11-86.71)	(86.58-86.74)	(86.31-86.57)	(85.97-86.39)	(85.55-86.86)
Numbers of cations in formula on the basis of 29 oxygen														
B	3.000	3.000	3.000	3.000	3.000	3.000	3.000	3.000	3.000	3.000	3.000	3.000	3.000	3.000
Na	0.782	0.657	0.557	0.570	0.448	0.839	0.598	0.587	0.558	0.474	0.763	0.572	0.517	0.512
Mg	1.121	1.561	2.466	2.423	2.344	2.101	2.032	2.174	1.984	2.054	1.758	2.138	2.308	1.885
Si	6.001	5.943	6.209	6.313	6.108	6.107	6.060	6.072	6.010	5.960	6.318	6.042	6.075	5.965
Al	5.947	5.920	3.829	3.503	4.612	5.249	5.212	5.187	5.623	5.593	4.897	5.383	5.214	5.555
K	0.018	0.022	0.061	0.063	0.023	0.009	0.015	0.011	0.020	0.026	0.019	0.023	0.015	0.022
Ca	0.076	0.214	0.404	0.396	0.531	0.127	0.379	0.374	0.345	0.454	0.168	0.378	0.439	0.388
Ti	0.076	0.101	0.217	0.218	0.217	0.160	0.118	0.117	0.037	0.033	0.154	0.056	0.084	0.060
Fe	1.824	1.410	2.713	3.042	1.819	1.139	1.602	1.490	1.349	1.36	1.886	1.410	1.343	1.574
Mn	0.004	0.007	0.012	0.007	0.000	0.002	0.006	0.004	0.004	0.006	0.006	0.006	0.003	0.002
K/K+Na+Ca	0.021	0.025	0.060	0.061	0.023	0.009	0.015	0.011	0.022	0.027	0.020	0.024	0.015	0.024
K/Na	0.024	0.034	0.110	0.110	0.052	0.011	0.025	0.019	0.036	0.055	0.025	0.04	0.029	0.043
Mg/Fe	0.615	1.107	0.909	0.797	1.288	1.161	1.268	1.458	1.471	1.509	0.932	1.517	1.718	1.197

*number of analysis **average

—Continuted

	N2-5		L-4		K1-7		L-7		HX-18		DN-12		HX-23	
	core (3)	rim (4)	core (4)	rim (2)	core (3)	rim (3)	core (3)	rim (3)	core (3)	rim (3)	core (3)	rim (2)	core (3)	rim (9)
Na_2O	1.634	1.632	1.231	1.195	1.908	1.871	1.693	1.141	2.196	2.012	1.964	2.062	2.254	2.158
	(1.341-1.838)	(1.453-1.875)	(1.062-1.708)	(0.051-1.340)	(1.899-1.913)	(1.809-1.919)	(1.491-1.821)	(1.091-1.143)	(2.017-2.392)	(1.967-2.038)	(1.824-2.049)	(2.053-2.071)	(2.211-2.347)	(1.980-2.338)
MgO	9.545	9.849	9.547	9.456	8.462	8.568	8.883	9.11	10.164	10.285	8.554	8.538	10.087	10.262
	(9.330-9.684)	(9.429-10.186)	(8.764-9.871)	(9.122-9.790)	(8.372-8.56)	(8.446-8.708)	(8.829-8.977)	(8.961-9.211)	(9.943-10.319)	(10.225-10.374)	(8.370-8.690)	(8.536-8.540)	(9.917-10.222)	(9.822-10.769)
SiO_2	36.164	36.420	34.22	34.093	35.465	35.489	36.051	35.367	36.516	36.492	36.169	35.825	36.589	36.807
	(35.702-36.548)	(36.164-36.733)	(3.968-34.511)	(33.749-34.438)	(35.350-36.616)	(35.357-35.625)	(36.048-36.054)	(35.233-35.569)	(36.501-36.534)	(36.250-36.651)	(36.127-36.233)	(35.548-36.102)	(36.441-36.749)	(36.643-36.966)
Al_2O_3	27.601	27.847	14.368	15.56	23.847	23.841	25.429	25.183	27.179	26.544	25.495	25.071	25.615	27.043
	(27.428-27.885)	(27.43-28.421)	(14.093-15.089)	(15.488-15.632)	(23.64-24.023)	(23.632-24.113)	(25.268-25.509)	(25.098-25.335)	(26.446-28.488)	(26.269-26.843)	(25.307-25.600)	(24.824-25.319)	(25.481-25.784)	(26.485-27.455)
K_2O	0.041	0.046	0.309	0.321	0.098	0.104	0.085	0.089	0.046	0.052	0.065	0.054	0.059	0.045
	(0.029-0.102)	(0.033-0.650)	(0.231-0.347)	(0.285-0.358)	(0.098-0.099)	(0.076-0.123)	(0.067-0.095)	(0.081-0.095)	(0.0342-0.0395)	(0.050-0.056)	(0.048-0.084)	(0.034-0.074)	(0.050-0.068)	(0.027-0.068)
CaO	2.423	2.473	2.751	2.84	2.097	2.171	2.389	3.361	1.768	2.209	1.932	1.848	1.544	1.813
	(2.189-2.812)	(2.156-2.914)	(1.790-3.129)	(2.625-3.055)	(2.016-2.170)	(2.096-2.224)	(2.258-2.643)	(3.207-3.484)	(1.387-2.096)	(2.072-2.119)	(1.829-2.005)	(1.836-1.859)	(1.436-1.675)	(1.660-2.060)
TiO_2	1.343	1.249	2.834	2.538	1.337	1.366	1.395	1.439	0.471	0.536	0.245	0.251	2.063	1.338
	(1.303-1.402)	(1.020-1.429)	(2.691-2.933)	(2.395-2.682)	(1.279-1.431)	(1.264-1.443)	(1.343-1.468)	(1.405-1.474)	(0.335-0.550)	(0.537-0.806)	(0.206-0.284)	(0.268-0.234)	(1.832-2.515)	(0.987-2.067)
FeO	6.923	6.683	20.267	18.659	12.749	12.915	10.501	10.457	7.341	7.962	12.076	12.428	7.68	6.838
	(6.818-7.057)	(6.601-7.046)	(19.560-20.759)	(18.459-18.860)	(12.683-12.832)	(12.488-13.183)	(0.378-10.611)	(10.359-10.571)	(6.367-8.224)	(7.624-8.163)	(11.855-12.238)	(12.406-12.450)	(7.526-7.833)	(5.893-7.527)
MnO	0.04	0.07	0.002	0.021	0.006	0.03	0.019	0.027	0.012	0.026	0.013	0.041	0.04	0.023
	(0.00-0.087)	(0.017-0.128)	(0.00-0.009)	(0.001-0.040)	(0.00-0.012)	(0.00-0.048)	(0.00-0.051)	(0.00-0.06)	(0.00-0.035)	(0.011-0.046)	(0.012-0.014)	(0.00-0.083)	(0.000-0.007)	(0.00-0.087)
Total	85.7	86.283	85.528	86.665	85.967	86.327	86.427	86.147	85.68	86.003	86.5	86.115	85.917	86.314
	(85.22-86.49)	(85.84-86.66)	(84.72-86.31)	(83.61-85.72)	(85.5-86.34)	(86.09-86.64)	(86.32-86.51)	(85.87-86.54)	(85.37-86.22)	(85.61-86.2)	(86.08-86.86)	(85.54-86.69)	(85.78-86.10)	(85.78-86.54)
Numbers of cations in formula on the basis of 29 oxygen														
B	3.000	3.000	3.000	3.000	3.000	3.000	3.000	3.000	3.000	3.000	3.000	3.000	3.000	3.000
Na	0.527	0.521	0.437	0.424	0.636	0.621	0.553	0.375	0.709	0.65	0.645	0.682	0.729	0.690
Mg	2.365	2.421	2.610	2.585	2.168	2.188	2.231	2.302	2.523	2.555	2.16	2.173	2.507	2.524
Si	6.011	6.006	6.275	6.251	6.096	6.082	6.073	5.996	6.081	6.082	6.126	6.116	6.101	6.071
Al	5.407	5.417	3.105	3.362	4.831	4.815	5.048	5.031	5.334	5.241	5.089	5.044	5.034	5.257
K	0.008	0.009	0.072	0.075	0.021	0.023	0.018	0.019	0.010	0.011	0.014	0.012	0.013	0.009
Ca	0.432	0.437	0.540	0.557	0.386	0.398	0.431	0.610	0.315	0.374	0.350	0.338	0.276	0.321
Ti	0.168	0.155	0.391	0.350	0.173	0.176	0.177	0.183	0.059	0.070	0.031	0.032	0.259	0.166
Fe	0.962	0.922	3.107	2.860	1.832	1.851	1.479	1.482	1.023	1.109	1.710	1.774	1.071	0.943
Mn	0.005	0.008	0.000	0.003	0.001	0.004	0.002	0.003	0.001	0.003	0.002	0.005	0.005	0.003
K/K+Na+Ca	0.009	0.010	0.069	0.071	0.020	0.022	0.018	0.019	0.010	0.011	0.014	0.012	0.013	0.009
K/Na	0.016	0.018	0.165	0.176	0.033	0.037	0.033	0.052	0.014	0.017	0.021	0.018	0.018	0.013
Mg/Fe	2.457	2.627	0.840	0.904	1.183	1.182	1.508	1.553	2.467	2.303	1.263	1.225	2.342	2.676

*number of analysis **average

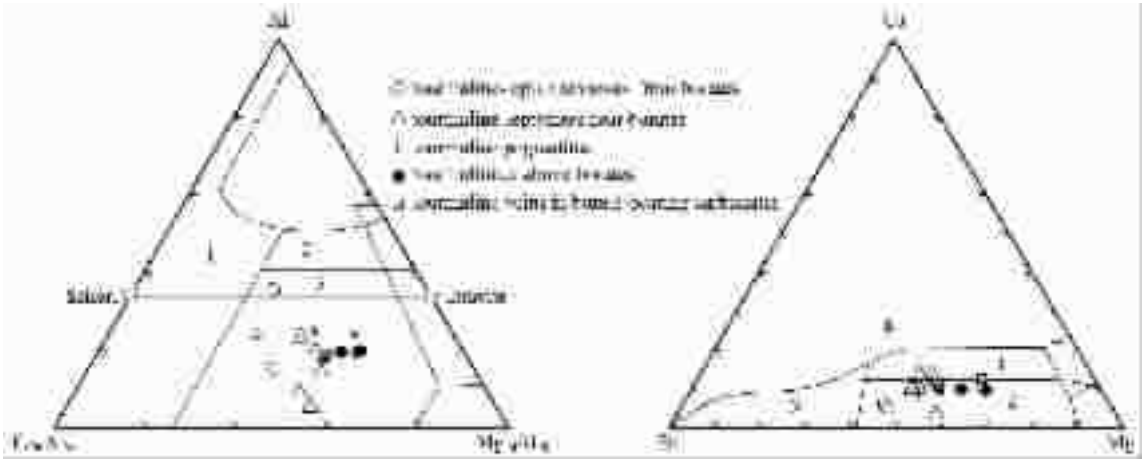

Fig. 4 Al−Fe−Mg and Ca−Fe−Mg plots of tourmaline

Areas after Henry and Guidotti (1985). Numbers in Al−Fe−Mg plot: 1−Li−poor granitoids and associated pegmtites; 2−Metapelites and metapsammites coexisting with an Al−saturated phase; 3−Metapelite and metapsammites not associated with an Al−saturated phase; 4−Fe^{3+}−rich tourmalinites, calc−silicates and metapelites. Numbers in Ca−Fe−Mg plot: 1− Ca−rich metapelites, metaspsammites and calc−silicates; 2− Ca−poor metapelites, metaspsammites and calc−silicates; 3− Li−poor granitoids and associated pegmtites; 4− Li−rich granitoids and associated pegmtites

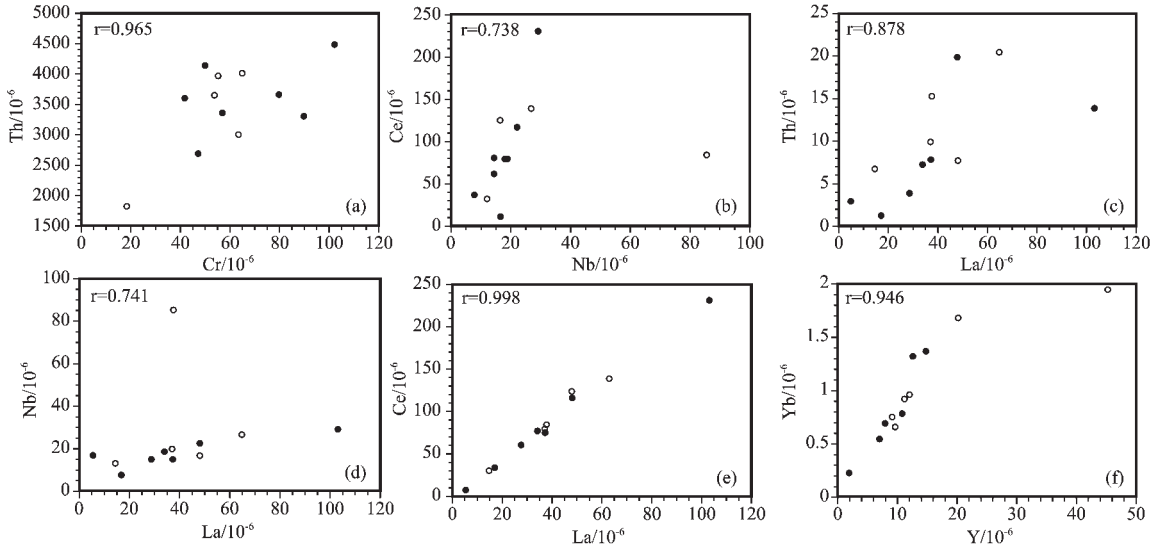

Fig.5 Trace element correlation plots of the stratiform tourmaline−rich rocks (solid circles) and their untourmalinised equivalents (open circles)

rich leptynites have higher K/Na than those in the albite−rich rocks (Table 2).

Optical zoning is not common, but simple zoning is seen in some tourmalines in the leptynites or tourmalinites. Chemical zoning is shown by several samples, mostly in the distal tourmaline. In most cases zoning is characterised by more schorl−rich cores and dravite−rich rims, which is more pronounced in the distal tourmaline−leptynites than in the proximal tourmalinites or tourmaline veins. The boundaries between the rims and cores vary from sharp to gradational.

4 Whole rock chemistry

Only the geochemistry of the tourmaline−bearing leptynites and stratiform tourmalinites is discussed here.

4.1 Major element geochemistry

There is a wide range of major element compositions. SiO_2 varies from 56% to 70% and $A1_2O_3$ and MgO levels decrease with increasing SiO_2 in the tourmalinised and untourmalinised leptynites and leptites(Table 3). In contrast, tourmaline concentration does not show a significant correlation with SiO_2[10], sug-

Table 3 Chemical analysis of the leptynites and the stratiform tourmaline-bearing and tourmaline-rich rocks

	H5-112	H1-43	La-12	H4-39	Wl-9	R11	R4Ⅰ-11	H5-60	H5-70*	H5-76*	H5-79*	Dc-10*	W1-6*
Major elements (%)													
SiO_2	56.01	66.72	62.66	57.91	62.36	63.50	69.31	73.37	63.69	72.27	70.48	65.59	73.93
Al_2O_3	15.99	15.19	13.99	18.01	15.41	13.01	12.86	14.23	18.28	14.80	10.80	14.33	7.53
Fe_2O_3	1.77	5.79	4.08	6.41	5.52	9.96	5.38	0.43	0.59	1.19	0.43	3.53	9.82
FeO	4.47	2.08	2.61	2.21	1.76	2.45	1.59	0.77	1.04	0.91	2.13	2.57	1.53
TiO	0.61	0.56	0.75	0.45	0.60	0.55	0.49	0.61	0.67	0.45	0.50	0.66	0.30
P_2O_5	0.10	0.07	0.15	0.01	0.12	0.01	0.08	0.31	0.12	0.10	0.09	0.17	0.10
MnO	0.09	0.02	0.04	0.06	0.17	0.04	0.03	0.03	0.04	0.11	0.09	0.11	0.13
CaO	0.53	0.60	1.19	3.18	0.43	0.95	0.90	2.17	0.95	0.86	1.83	0.31	0.32
MgO	7.89	3.64	4.29	7.35	1.82	3.01	3.53	0.79	1.34	0.80	5.59	2.65	0.51
K_2O	11.15	30.16	7.30	0.10	10.52	3.66	3.10	0.88	8.83	2.05	2.97	5.31	5.66
Na_2O	0.86	3.04	1.23	1.12	1.10	1.23	1.16	5.98	4.21	6.46	3.95	3.99	0.34
Los	1.11	1.52	1.13	2.78	0.42	1.01	0.93	0.92	0.57	0.45	0.57	0.38	0.26
Trace elements (10^{-6})													
Cr	80.4	57.8	103	47.7	42.3	90.5	50.4	54.2	65.4	42.7	63.8	55.7	18.7
Rb	320	4.31	114	1.73	374	67.3	36.6	24	147	27.2	164	418	168
Sr	145	123	157	320	134	217	171	136	79.7	39.4	199	316	97.9
Ba	615	40	444	14	1458	135	383	219	897	331	174	1555	3872
Zr	254	223	260	261	186	210	200	438	329	302	196	1199	63.8
Hf	7.50	3.70	4.10	5.30	15.10	8.00	6.00	4.10	5.00	11.70	5.00	15.10	6.30
Nb	29.9	15.5	15.5	17.5	23.1	8.49	19.4	17.2	27.4	25.4	20	85.5	13.2
Ta	3.40	3.40	3.10	3.10	2.00	3.50	3.30	3.00	3.70	3.00	2.90	1.20	1.00
Th	14.01	8.01	4.02	3.26	19.91	1.34	6.95	7.69	20.49	8.95	8.95	15.35	6.68
La	103.6	37.67	29.03	5.73	48.77	17.77	34.61	48.21	65.23	37.53	37.53	37.99	14.79
Ce	230.2	80.8	62.11	10.93	117.5	37.09	79.99	125.2	138.66	79.37	79.37	85.53	31.06
Nd	67.56	25.22	23.12	3.69	39.53	15.51	28.87	42.29	45.96	25.34	25.34	28.28	12.46
Sm	8.97	3.85	3.32	0.46	6.05	2.91	6.01	7.04	8.84	3.27	3.27	4.27	1.94
Eu	2.28	0.52	0.98	0.09	2.42	0.71	1.09	2.49	2.64	0.70	0.70	2.16	3.32
Gd	15.94	6.76	6.64	0.91	10.7	4.03	8.64	11.36	12.35	6.15	6.15	5.27	3.03
Yb	1.37	0.71	0.80	0.26	0.93	0.55	1.33	1.68	1.95	1.01	0.75	0.66	0.97
Lu	0.19	0.10	0.10	0.05	0.13	0.10	0.22	0.19	0.35	0.11	0.11	0.04	0.12
Y	15.19	8.51	11.25	2.05	11.72	7.50	12.90	20.40	45.31	9.55	9.55	10.05	12.49

*untourmalinised leptynites

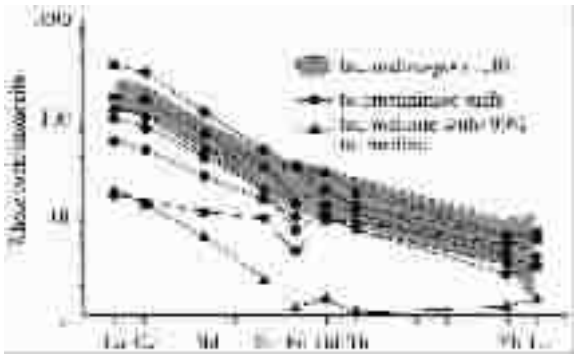

Fig.6 Chondrite-normalised REE patterns of the tourmaline-rich rocks and tourmaline-poor leptynites

gesting that high boron levels arose from addition of boron to the rocks rather than being inherited from enrichments in acidic protoliths.

4.2 Trace element geochemistry

Elements generally considered to be immobile during water-rock interaction show good correlations between their concentrations in the tourmaline-rich rocks (including the tourmalinites) and the untourmalinised leptynite and leptite equivalents (Fig. 5). Again, this suggests that the tourmaline formed by selective replacement of Al-rich layers in the original tuffs by boron-rich hydrothermal fluids. Due to Nb and Ti anomalies a small number of samples do not fit the trends on Nb-Ce, Nb-La and La-Ti diagrams, which have lowered the correlation coefficients (Fig.5-b, 5-c, and 5-d). This could be due to heterogeneous distributions of Nb- and Ti-hosting acessory minerals in the pyroclastic rocks, which do not host much HFSE. Similar behaviour has been seen elsewhere in tourmalinites hosted by clastic sediments[5,21].

The rare earth element (REE) patterns of the tourmaline-rich rocks are also similar to those of the metamorphosed pyroclastic rocks (Fig. 6). The more pronounced negative Eu anomalies of the tourmaline-rich rocks may reflect a breaking down of plagioclase during the tourmalinisation.

5 Boron isotope geochemistry

Boron isotope ratios were analysed in borates and tourmaline mineral separates from the area using the methods described by Palmer and Slack[22]. The results are listed in Table 3 and are expressed in terms of $\delta^{11}B$ values, where:

$$\delta^{11}B = \{ [(^{11}B/^{10}B_{sample})/(^{11}B/^{10}B_{standard})] - 1 \} \times 10^3$$

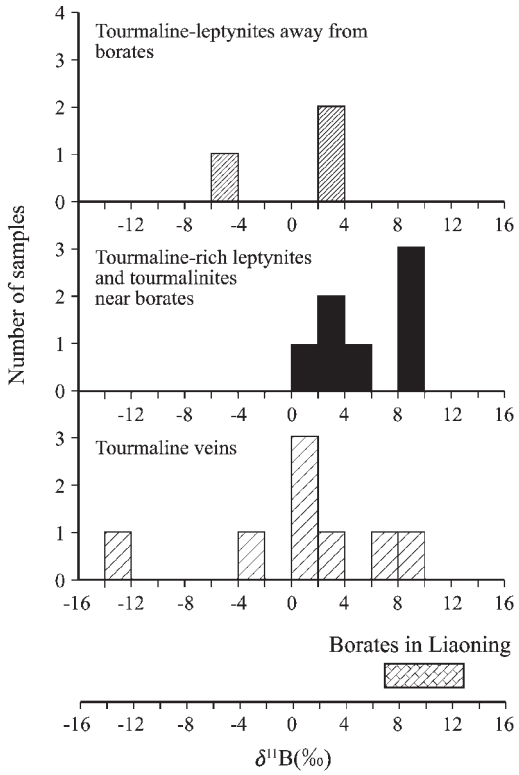

Fig.7 $\delta^{11}B$ histograms of tourmalines from the evaporitic sequence. Boron isotope composition range of borates is given for comparison

The standard is NBS boric acid SRM951. Approximately 100 analyses of this standard at Bristol yielded an average $^{11}B/^{10}B$ ratio of 4.0529 (±0.12‰, 0.2σ).

The borates have a relatively narrow $\delta^{11}B$ range of +7.5 ‰ to +13.0 ‰ (Peng and Palmer, 1995 and unpublished data). The $\delta^{11}B$ values of tourmalines span a wider range, from −12.4 ‰ to +9.4 ‰ (Table 4, Fig. 7).

Tourmalines from tourmaline−leptynites and stratiform tourmalinites proximal to the borates have $\delta^{11}B$ values of +1.8 ‰ to +9.3 ‰,slightly lower than those of the underlying borates. Tourmalines from distal leptynites show lower $\delta^{11}B$ value s (−5.2‰ to +3.6 ‰), with the lowest value (−5.2 ‰) occurring in fine−grained tourmaline that shows textural evidence of a metamorphic origin from boron−enriched sediments (sample LN−14).Tourmaline from the quartz−tourmaline veins and pegmatites have more variable $\delta^{11}B$ values (−12.4 ‰ to +9.4 ‰). In general, tourmalines from the pegmatites have lower $\delta^{11}B$ values than those from the quartz−tourmaline veinlets in the borate−carbonates, although low $\delta^{11}B$ values (+1.3 ‰) are found in quartz −tourmaline veins with associated phlogopite (sample H5−92).

6 Discussion

6.1 Comments on the previous models for of the origin tourmaline−rich rocks

There have been several models for the origin of the tourmaline−rich rocks associated with the Liaoning and Jilin borate deposits. The tourmaline has been described as the product of metasomatism associated with intrusion of granites [7,14], boron−rich acidic lavas [15,23]; chemical sediments resulting from seafloor hydrothermal plumes[24], and boron−rich argillaceous sediments .

A granitic origin for the tourmaline is not appropriate for several reasons. Firstly, tourmaline in the stratiform tourmalinites and leptynites formed mostly during regional metamorphism (S_1), predating the emplacement of the granites. Secondly, A−type granites are not generally boron−rich and rarely contain high tourmaline concentrations. This contrasts with S−type granites

Table 4 Boron isotopic composition of tourmaline

	$\delta^{11}B$ (‰)		Location and description
Tourmalintes and tourmaline-bearing leptynites form the hanging wall			
H4-49	+5.8±0.3	+6.0±0.3	Tourmalinite, Zhuanmiao
LN36	+9.0±0.3	+9.6±0.3	Tourmaline-microcline leptynite, Zhuanmiao
LN-38	+8.1±0.4	+8.3±0.4	Tourmaline-microcline leptynite, Zhuanmiao
LA-12	+8.8±0.2	+8.9±0.4	Tourmaline-microcline leptynite, Zhuanmiao
H5-112	+1.8±0.3	+1.8±0.2	Tourmaline-microcline gneiss, Huayuangou, Zhuanmiao
R-11	+2.4±0.2	+1.9±0.2	Tourmaline, Errengouo
LN-31	+3.2±0.4	+2.5±0.5	Tourmaline-microcline leptynite, Zhuanmiao
Tourmaline veins from hanging wall and borate-bearing carbonates			
LN34	+7.5±0.4	+6.6±0.3	Tourmaline vein in borate-carbonates, Zhuanmiao
LN35	+9.2±0.3	+9.6±0.4	Tourmaline quartz vein in borate-carbonates, Zhuanmiao
LN-37	+0.5±0.4	+0.9±0.2	Tourmaline pegmatite in borate-carbonates, Zhuanmiao
LN-21a	+3.2±0.4	+2.4±0.3	Tourmaline-phlogopite vein in borate-carbonates, Wengquangou
LN-21b	+1.3±0.4	+1.1±0.4	Tourmaline quartz vein, Wengquangou
LN-15	-12.3±0.2	-12.4±0.3	Felsic vein with trace tourmaline in hanging wall amphibole leptynites, Wengquanggou
LN21c	-4.0±0.4	-3.1±0.3	Tourmaline-pyrite quartz vein in borate-carbonates,Wengquangou
LH5-92	+1.3±0.4	-0.2±0.4	phlogopite-rich rocks in carbonates,rimming pegmatite,Zhuanmiao
Tourmaline-bearing leptynites away from the borate bodies			
LN-13	+2.8±0.2	+2.4±0.2	Tourmaline-leptynite, Lugong
LN14	−5.2±0.3	−5.2±0.4	Tourmaline-leptynite (mostly early, fine-grained tourmaline), Lugong
H1-43	+4.0±0.2	+3.6±0.4	Tourmaline-albite leptynite, Zhuanmiao

that are often associated with extensive tourmalinisation in the granites and country rocks[25~27]. Thirdly, significant occurrences of tourmaline related to granites are often accompanied by polymetallic mineralisation, e.g., Sn and W. In the Liaoning area there is no significant mineralisation of this type either within or adjacent to the granites. Lastly, the tourmaline-bearing felsic pegmatites are related to the granite, but they are only tourmaline-bearing where they crosscut the borate bodies. In these cases tourmaline is present in the rims of the pegmatites and appears to have formed by boron diffusing into the pegmatite from the borates. Felsic veins and pegmatites in the footwall of the borates and within the granites themselves only contain sparse tourmaline. These observations suggest that tourmaline in the felsic veins and pegmatites was derived primarily from the borates during emplacement of the granites, rather than from granitic melts.

An acidic volcanic protolith is not supported by the field evidence or geological studies. The sedimentary bedding in the tourmaline-rich leptynites precludes a lava precursor. The lack of a significant correlation between B and Si concentrations contrasts to that expected in an acidic magmatic differentiation trend [10].

Marine sediments have boron concentrations up to $2\ 000\times10^{-6}$ [28], but these are insufficient to account for the presence of tourmaline-rich layers and tourmalinites as diagenesis and/or metamorphism of such clays only produce a few percent tourmaline in the rocks [2~3,5], whereas up to 50% tourmaline is observed in some rock units of Liaoning and Jilin. However, the tourmaline in leptynites containing <5% tourmaline, which are continuous throughout the study area may have formed by adsorption of boron to clay-rich sediments. This is consistent with the textural evidence that the tourmaline formed earlier than most other metamorphic minerals (Fig.3-A).

Boron is enriched in submarine and subaerial hydrothermal waters[29~30] and boron-rich fluids are involved in the formation of stratiform tourmalinites. However, hydrothermal fluids do not contain sufficient Al to produce large volumes of tourmaline on their own [5]; hence the formation of tourmalinites requires that they form by replacement of Al-rich protoliths rather than by direct precipitation from fluids [2,5,21].

6.2 Timing of the tourmalinisation

Field and structural evidence indicates that tourmalinisation took place both during and after the peak regional metamorphism. Tourmalines in the tourmaline-leptynites and stratiform tourmalinite layers have granoblastic textures and are oriented parallel to S_1. These suggest that they formed during or before the syntectonic, peak metamorphism. The small tourmaline grains enclosed within quartz and feldspars in the leptynites (Fig. 3) suggest an earlier, less volumetric, formation of tourmaline. Some of these small tourmaline grains may be of detrital origin, but the lack of sharp core boundaries and the absence of other associated heavy minerals (e.g., zircon and ilmenite) suggest that they are authigenic. One possible interpretation is that they represent boron enrichment via clay adsorption during deposition and diagenesis of the borates. In this scenario, adsorbed boron was released from the clay minerals (that were later metamorphosed to form biotite and/or other silicates) during diagenesis/early metamorphism to form small amount of authengenic tourmaline. This process is relatively common in boron-rich metamorphic sediments [31~33]. This hypothesis is supported by the close association between tourmaline and biotite layers in the leptynites. The coarser tourmaline grains account for >90% of the total tourmaline in the rocks and are intergrown with quartz and feldspars. This later generation of tourmaline represents more extensive hydrothermal boron enrichment that overprinted the earlier tourmaline, as suggested by their textural relationship (Fig.3-A). The two processes were continuous within the same metamorphic-tectonic episode. The identification of the two generations is easier in rocks distal to the borate bodies. In the immediate hanging walls of borate bodies, the tourmaline is dominated by the extensive tourmalinisation of the second generation.

The pegmatites and tourmaline veins in different lithologies all crosscut S_1, and are associated with the A-type granites. Their textures suggest a hydrothermal origin, similar to the granite-related tourmalinisation found in many Sn-W deposits [34]. The irregular quartz-tourmaline veins and tourmaline-pegmatites are controlled by the same fracture system and are spatially associated with one another, with the former surrounding the latter. This indicates that they formed during the same post-tectonic hydrothermal event that is related to the granite emplacement.

6.3 Sources of boron

The intimate spatial and temporal relationship between the tourmaline-rich rocks and the borate bodies suggest a genetic link between them, i.e., the borates acted as the source of boron in the overlying tourmalines, and the boron-rich fluids that precipitated borates may also have contributed boron to the clay-rich sediments (tuffs). Non-marine evaporites can contain high boron concentrations [6]and they are readily leached of this boron by circulating hydrothermal fluids, as shown in the modem Salton Sea geothermal field [35]. Boron-rich evaporites and

evaporitic sequences have been identified in Precambrian terranes elsewhere, e.g., Broken Hill, Australia[4~5,23]and Barberton, South Africa [13]. Hence, the classification of the Liaoning borate deposits as evaporites is consistent with their geological and geochemical setting[12], and their role as a source of boron for the associated tourmaline-rich rocks.

The use of the $\delta^{11}B$ value of tourmaline to calculate that of the original fluids requires that there is no boron loss from the rock system during metamorphism, as this would produce lighter $\delta^{11}B$ values in the reprecipitated tourmaline than the original rocks [22]. The restriction of tourmaline-rich rocks to unit 3 and the absence of high boron concentrations outside this unit suggest there was not substantial release of boron from metamorphically recrystalised tourmaline. Hence, the tourmalines may record the original $\delta^{11}B$ of fluids from which they formed. As hydrothermal fluids circulate through sediments boron is leached from the host rocks with no apparent isotope fractionation[30,36~37]. During formation of tourmaline from aqueous fluids the light isotope,^{10}B,is enriched in the tourmaline[22]with the degree of isotope fractionation being temperature dependent[38].

The three principal borate minerals (suanite, szaibelyite and ludwigite) are not primary evaporite minerals found in unmetamorphosed borate deposits [6].The textural and geochemical evidence suggest that these minerals were originally hydrated Mg-borate minerals, such as inderite and pinnoite, that were dehydrated during progressive metamorphism to form suanite and ludwigite and partially rehydrated during retrograde metamorphism to form szaibelyite [12]. Boron is very mobile during water-rock interaction, so during dehydration reactions it is likely that some boron was lost from the borates. This would lower the $\delta^{11}B$ of the residual borates[22,30].

The tourmalines have $\delta^{11}B$ values in the range −14‰ to +10‰, which are lower than those of the borates (Fig.7, Table 4). The $\delta^{11}B$ values of tourmaline from tourmalinites and tourmaline-rich rocks near the borates range from +1.8‰ to +9.3 ‰ (average 5.9 ‰), slightly lower than those of the borates (+7.5‰ to +13.0 ‰). If the borates were the principal source of boron for the tourmalines the offset in $\delta^{11}B$ values of 4.6 ‰ implies an average temperature of formation of 500-550 ℃ for the tourmaline [38], with 700℃ as the upper limit. The peak metamorphism temperature, calculated via garnet-biotite (gneissis from the Gaojiayu Formation) and hornblende-plagioclase (from amphibolites in the borate deposits) geobarometers, was 650-750℃ (D.Q. Hu, 1994, pers. commun.). This is consistent with the textural evidence that tourmaline formed before the peak metamorphism and was recrystalised during metamorphism.

Distal tourmalines have lower $\delta^{11}B$ values (−5.2‰~+3.8 ‰, average +0.7 ‰). If the boron also came from the borates, this would imply a lower temperature of tourmaline formation. The sample with predominant pre-metamorphic boron-enrichment (LN-14) has the lowest $\delta^{11}B$ value (−5.2 ‰), which gives an offset in $\delta^{11}B$ values of 15 ‰, indicating a maximum temperature of formation of 200-300℃ [38]. Although it should be noted that the $\delta^{11}B$ of the borates may have been lowered during metamorphism, and would imply an even lower temperature for the formation of tourmaline. It is also possible that the fluids precipitating the early tourmaline had lower $\delta^{11}B$ values.

The similar HFSE and REE patterns of tourmalinites and their untourmalinised equivalents suggest that the tourmalines formed via replacement of the tuffs by boron-rich fluids leached from the evaporite. A chemical comparison between these two sets of rocks indicates that the former have higher B, Fe and K concentrations than the latter, with Si and Al levels substantially the same [11]. The higher K in the tourmalinites may be due to K-Na zoning in the tuffs[11], as the borates are usually enclosed by a K-rich zone. Mg/Fe and K/Na ratio variations of the tourmalines and their zoning are also compatible with their host lithologies (Table 2). Proximal tourmalines have higher Mg/Fe and K/Na ratios and the rims are generally more Mg-rich than the cores. The premetamorphic fine-grained tourmaline has a significantly higher schorl component than the latter, syn-metamorphic tourmaline. These observations may reflect the evolution of fluid chemistry: the early tourmaline formed by uptake of Fe, Al, Si and B from the sediments (clay-rich) and as the later evaporite-derived fluids were Mg-rich, the Mg/Fe ratio of the tourmaline increased. Tourmalines from veins and pegmatites have a wider range of $\delta^{11}B$ values than the stratiform tourmalinites and tourmaline leptynites (Fig.7). This could be because they cut through diverse lithologies and have obtained boron from different sources. A correlation exists between the $\delta^{11}B$ values of the tourmaline veins and borates. Borates from Wengquangou have lower $\delta^{11}B$ values than those from the other districts and the $\delta^{11}B$ values of the tourmalines are also significantly lower (Table 4). Tourmaline-rich quartz veins (e.g., sample LN-35 from Zhuanmiao, with $\delta^{11}B$ value of +9.4 ‰) from the borate-carbonates have $\delta^{11}B$ values closer to that of the associated borates (+10‰ to+11 ‰ in the district, Peng and Palmer unpublished data), suggesting that boron was largely derived from the borates. Tourmalines from the pegmatites have much lower $\delta^{11}B$ values (−12.4‰ to +0.9 ‰). Fluid inclusion studies of these pegmatites yield homogenisation temperatures of ~300℃ (Y.Wang, 1993, pets. com.), which could be the lower limit of the temperature of formation. This indicates $\delta^{11}B$ values of up to −3% to +9 % for the fluids [38]. This suggests that the pegmatites contain a mixture of boron derived from a continen tal crustal source, whose $\delta^{11}B$ averages −5 ‰ [39], and boron

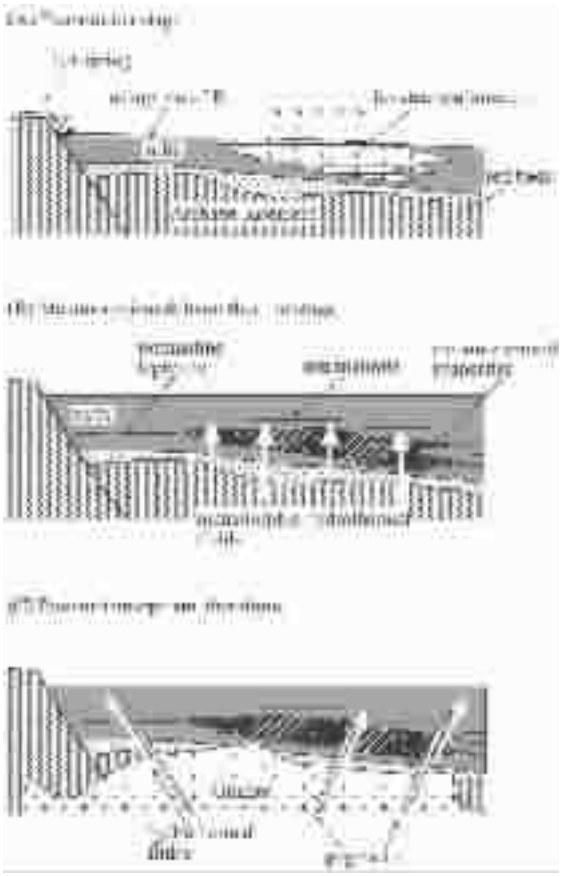

Fig.8 A genetic model for the origin of tourmalines in the evaporitic sequence. For details see text

leached from the borates, with $\delta^{11}B$ values of +10 ‰. A continental crustal source signature is better expressed in pegmatite with very low tourmaline content, e.g., sample LN-15 contains only trace tourmaline and yields $\delta^{11}B$ of -12 ‰. This is compatible with the low boron concentration in the footwall rocks.

7 Conclusions

There is a clear spatial and temporal link between the occurrence of tourmaline-rich rocks and borate deposits in the Liaoning and Jilin areas. A comparison of trace element patterns between the stratiform tourmaline-rich and their untourmalinised equivalents suggests that the former is the replacement of the latter.

These observations suggest a three-stage model for formation of tourmaline in the Liaoning and Jilin areas(Fig.8):

Stage 1: During deposition and diagenesis of borate evaporites, clay-rich sediments adsorbed boron from saline water, boron-rich springs or fluids released during diagenesis of the borates. The boron was released during diagenesis-early metamorphism (at temperatures of <200 to 300℃), to form the small tourmaline grains that were subsequently enclosed by other metamorphic minerals (Fig.3-A).

Stage 2: During prograde metamorphism, higher temperature (400-500℃) fluids leached boron from the borates. These boron-rich fluids passed though the overlying tuffs and reacted with the clay-rich layers to form tourmaline overgrowths on the stage 1 tourmaline (Fig.3-B) and was recrystallised at peak metamorphic temperatures (650-700℃).

Stage 3: Postdating the peak metamorphism, A-type granites intruded the sequence. Hydrothermal systems initiated by these granites leached boron from the borates and, to a lesser extent, from clastic sediments. As a result tourmaline was precipitated close to the margins of the pegmatites (Fig.3-C).

The observation that significant volumes of tourmaline are produced from the remobilisation of boron from borate deposits has implications for the occurrence of tourmaline in other ancient sedimented rift settings.Involvement of borate-bearing evaporites has been invoked for the origin of tourmalinites associated with some giant massive sulfide deposits and has implications for the transport and deposition of metals in the ore deposits[5,40].

Acknowledgements: The work is sponsored by National Natural Science Foundation of China (No49573175,40373023) and the British Royal Society that financed the Sino-British joint project on the geochemistry of the borate deposits in China. The authors are grateful to Liu Jingdang for his tremendous help during the field trip to the deposits.

References:

[1] Slack J F.Tourmaline in Appalachian-Caledonian massive sulfide deposits and its exploration significance [J]. Inst. Mining. Metall. Trans. 1982,9 lB: 81~89.

[2] Slack J F, Herriman N, Barnes R G, et al. Stratiform tourmalinites in metamorphic terranes and their geological significance[J]. Geology, 1984, 12:713~716.

[3] Plimer I R. Tourmalinites associated with Australian Proterozoic exhalative ores[A]. In: Friedrich G H, Herzig P M (eds.).Base Metal Sulfide Deposits in Sedimentary and Volcanic Environments. Berlin: Springer-Verlag, 1988. 255~283.

[4] Slack J F, Palmer M R,Stevens B P J. Boron isotope evidence for the involvement of nonmarine evaporite in the origin of the Broken Hill ore deposit[J]. Nature, 1989, 342: 913~916.

[5] Slack J F, Palmer M R, Stevens B P J, et al. Origin and significance of tourmaline-rich rocks in the Broken Hill district, Australia[J]. Econ. Geol., 1993, 88: 505~544.

[6] Kistler R B, Helvaci C. Boron and borates[A]. In: Carr D D (ed.). Industrial Minerals and Rocks, Society of Mining, Metallurgy and Exploration[C]. 1994, 171~186.

[7] Wang X Z, Xu X Y. Formation conditions of szaibelyite skarn deposits[J]. Sci. Geol. Sin., 1964, 2: 157~171.

[8] Feng B. Origin of the borate deposits hosted in the Precambrian metamorphic rocks, Liaoning, China[A]. In: Abstr. Conf. Chinese Geol. Soc. [C]. 1962.

[9] Zhang Q S. Early Proterozoic tectonic styles and associated mineral deposits of the north China Platform[J]. Precamb. Res., 1988,39: 1~29.

[10] Peng Q M, Feng B Z, Liu J D, et al. Geology of the early Proterozoic boron deposits in eastern Liaoning, Northeastern China [J]. Resource Geology, 1993, 15:343~350.

[11] Peng Q M,Xu H.The Paleoproterozoic Meta-evaporitic Sequence and Boron Deposits in Liaoning-Jilin [M]. Changchun:Northeast Normal University Press, 1994.122 (in Chinese with English abstract).

[12] Peng Q M, Palmer M R. The Paleoproterozoic boron deposits in eastern Liaoning, China: a metamorphosed evaporite[J]. Precamb. Res., 1995,72: 185~197.

[13] Byerly G R, Palmer M R. Tourmalinisation in the Barberton greenstone belt, South Africa: early Archean metasomatism by evaporite-derived boron[J]. Contrib. Mineral. Petrol. 1991,107: 387~402.

[14] Wang X Z. Conditions for formation of the endogenetic szaibelyite skarn deposits[J]. Sci. Geol. Sin. 1965, 3: 295~297.

[15] Zhang Q S. Geology and Metallogeny of the Early Precambrian in China[M]. Changchun:Jilin People´ s Press, 1984. 536 (in Chinese with English abstract).

[16] Jiang C C. The Precambrian of Eastern Liaoning and Jilin [M]. Shenyang: Liaoning Sci. Tech. Press, 1987 (in Chinese with English abstract).

[17] Sun M, Armstrong R L, Lambert R S J, et al. Petrochemistry and Sr, Pb and Nd isotopic geochemistry of the Paleoproterozoic Kuandian Complex, the eastern Liaoning Province, China[J]. Precamb. Res., 1993, 62:171~190.

[18] Wang R Z. Isotopic dating of the lower Proterozoic in Liaoning and Jilin areas[A]. In: Bai J (ed).Geology and Pb-Zn Mineralisation in the Northern Margin of North China Platform[C]. Beijing: Geological Publishing House, 1993. 22~25.

[19] Peng Q M,Palmer M R. The Paleoproterozoic Mg and Mg-Fe borate deposits of Liaoning and Jilin Provinces, Northeast China [J]. Economic Geology, 2002, 97:93~108.

[20] Fisher R V, Schminke H U. Pyroclastic Rocks[M]. Berlin: Springer-Verlag, 1984,472.

[21] Bandyopadhyay B K, Slack J F, Palmer M R, et al. Tourmalinites associated with stratabound massive sulfide deposits in the Proterozoic Sakoli Group, Nagpur district, central India[A]. In:Proc. 8th IAGOD Symp[C]. 1993. 867~885.

[22] Palmer M R, Slack J F. Boron isotopic composition of tourmaline from massive sulfide deposits and tourmalinites[J]. Contrib. Mineral. Petrol. 1989, 103: 434~451.

[23] Li S Y. The bi-model volcanism and magma differentiation in the Liao-Ji paleo-rift[J]. J. Changchun Uni. Earth Sci., 1994, 24: 143~147 (in Chinese with English abstract).

[24] Zou R,Feng B Z.Characteristics and origin of the tourmalinites in the early Proterozoic boron-bearing series, Liaoning and Jilin [J]. J. Changchun Uni. Earth Sci., 1993,23:373~380 (in Chinese with English abstract).

[25] Manning D A C, Pichavant M. The role of fluorine and boron in the generation of granitic melts[A]. In: Atherton M P, Gribble C D (eds.). Migmatites, Melting and Metamorphism[C]. Siva, Nantwich, 1983, 93~109.

[26] Peng Q M. Geology and genesis of the Proterozoic tin deposit at Chahe, Sichuan[J]. J. Changchun Uni. Earth Sci., 1987, 14:179~187 (in Chinese with English abstract).

[27]Pitcher W S. The Nature and Origin of Granite [M].London: Blackie Academic, 1993, 321.

[28] Harder H. Boron contents of sediments as a tool in facies analysis[J]. Sedimentary Geol., 1970,4: 153~176.

[29] Ellis A J,Mahon W A J.Chemistry and Geothermal Systems [M]. London: Academic Press, 1977.

[30] Palmer M R. Boron isotope systematics of hydrothermal fluids and tourmalinites: A synthesis[J]. Chem. Geol. (Isotop. Geosci. Sect.) 1991,94:111~121.

[31] Henry D J, Guidotti C V. Tourmaline as a petrogenetic indicator mineral: an example from the staurolite-grade metapelite of NW Maine [J]. American Mineralogist, 1985, 70:1~15.

[32] Michalidis K, Kassoli-Fournaraki A. Tourmaline concentrations in migmatitic metasedimentary rocks of the Riziana and Kolchiko areas in Macedonia, northern Greece [J]. European J. Mineral., 1994, 4: 557~569.

[33] Michalidis K, Kassoli-Fournaraki A,Detrich R V. The origin of zoned tourmalines in graphite-rich metasedimentary rocks from Macedonia, Northern Greece[J]. European J. Mineral., 1996, 8: 393~404.

[34] Taylor R G.Geology of tin deposits (Developments in economic geology) [J]. Amsterdam: Elsevier, 1979, 11:543.

[35] McKibben M A, Williammms A E, Okubo S. Metamor phosed Pliocene evaporites and the origin of hypersaline brines in the Salton Sea geothermal system, California:fluid inclusion evidence[J]. Geochim. Cosmochim. Acta ,1988, 52: 1047~1056.

[36] Spivack A J, Edmond J M. Boron isotope exchange between sea water and the oceanic crust[J]. Geochim. Cosmochim. Acta, 1987,51: 1033~1043.

[37] Spivack A J, Palmer M R ,Edmond J M. The sedimentary cycle of the boron isotopes[J]. Geochim. Cosmochim. Acta, 1987, 51: 1939~1949.

[38] Palmer M R, London D, Morgan G B, et al. Experimental determination of fractionation of $^{11}B/^{10}B$ between tourmaline and aqueous vapour: A temperature and pressure dependent isotope system[J]. Chem. Geol. (Isotope Geol. Sect.), 1992,101: 123~130.

[39] Chaussidon M, Albarede F. Secular boron isotope variations in the continental crust: An ion microprobe study [J]. Earth Planet Sci. Lett., 1992, 108:229~241.

[40] Hoy T. The age, chemistry and tectonic setting of the Middle Proterozoic Moyie sills, Purcell Supergroup, Southeastern British Columbia[J]. Ca. J. Earth Sci., 1989,26: 2305~2317.

辽宁古元古代地体中富电气石岩石的成因:蒸发岩硼源的证据

许　虹[1]　彭齐鸣[2]　Martin R. Palmer[3]

(1.中国地质大学,北京 100083; 2.中国地质调查局, 北京 100011;
3. School of Ocean & Earth Science, University of Southampton, UK)

提要:辽宁东部古元古界底部地层(南辽河群)中赋存着大型的硼酸盐矿床,含矿层位中广泛分布含电气石的变粒岩和电英岩。空间上这些含电气石的岩石与硼酸盐有着密切的联系,电气石可以作为区域硼矿找矿的标志。已有研究结果表明,该地区的硼酸盐矿床是变质蒸发岩成因。本研究对该区不同产状的电气石和硼酸盐的地质特征,全岩和矿物成分、硼同位素组成进行了分析。本区的电气石包括层状和脉状两大类,而电气石的富集与硼酸盐关系密切,电英岩往往分布在硼酸盐矿体的上盘。而矿体的下盘一般不产出富电气石的岩石。当长英质脉体穿过硼酸盐矿体时,脉体中往往会富集电气石。含电气石岩石的全岩地球化学分析表明,它们的 REE 及其他微量元素特征以及相关性关系与周围不含电气石的同类岩石十分相似,反映出一种成因上的联系。本区电气石主要属于镁电气石—铁电气石系列,靠近硼矿体的电气石比远离硼矿体的电气石更加富镁,有着更高的 Mg/Fe 比值。电气石和硼酸盐的硼同位素成分分析显示出二者在同位素组成上的相似性,前者比后者的 $\delta^{11}B$ 稍低,这可能是由于热液活动过程中同位素分馏的结果。电气石的硼同位素组成在空间上显示出变化规律:远离硼酸盐矿体的电气石的 $\delta^{11}B$ 值(−5.2 ‰~ +3.6 ‰)比矿体附近的电气石低(平均 +10.5 ‰)。以上空间和成分上的关系表明硼酸盐可能是形成电气石主要的硼来源,电气石是在热液过程中通过淋滤下伏含硼蒸发岩中的硼形成含硼热液,在与上覆沉积物交代过程中形成含电气石岩石。电气石的条带是热液顺层选择交代的结果。本区电气石与硼酸盐的关系表明,层状电气石可以通过含硼热液交代的方式形成。变质地体中的层状电气石岩石的出现可能与变质蒸发岩有关。这一认识对区域硼矿勘查工作和变质地体的沉积环境分析有借鉴意义。

关　键　词:电气石;硼酸盐;古元古代;蒸发岩;辽宁

中图分类号:P578.953;P578.93　　**文献标识码**:A　　**文章编号**: 1000−3657(2004)03−0240−014